International Journal of Pharmaceutics 424 (2012) 128–137

Contents lists available at SciVerse ScienceDirect

International Journal of Pharmaceutics

journal homepage: www.elsevier.com/locate/ijpharm

Pharmaceutical nanotechnology

Loading hydrophilic drug in solid lipid media as nanoparticles: Statistical modeling of entrapment efficiency and particle size

Maryam Ghadiri[a], Shohreh Fatemi[a,*], Alireza Vatanara[b,**], Delaram Doroud[b], Abdolhossein Rouholamini Najafabadi[b], Majid Darabi[b], Amir Abbas Rahimi[c]

[a] School of Chemical Engineering, College of Engineering, University of Tehran, P.O.Box 11155-4563, Tehran, Iran
[b] Department of Pharmaceutics, School of Pharmacy, Tehran University of Medical Sciences, Tehran, Iran
[c] Nanobiotechnology Department, Pasteur Institute of Iran, Tehran, Iran

ARTICLE INFO

Article history:
Received 9 September 2011
Received in revised form
18 December 2011
Accepted 21 December 2011
Available online 30 December 2011

Keywords:
Paromomycin
Solid lipid nanoparticles
Entrapment efficiency
Statistical modeling

ABSTRACT

Solid lipid nanoparticle (SLN) is a very well tolerated carrier systems for dermal application due to the employment physiological and/or biodegradable lipids. The effects of five factors, two categorical and three quantitative factors, were studied on the mean diameter and entrapment efficiency of the produced SLNs using response surface method (RSM), D-optimal design. Two methods of microemulsion and solvent diffusion and two types of lipid, cetyl palmitate and stearic acid, were examined comparatively. The quantitative variables were studied in three levels; amount of original Paromomycin (60, 90 and 120 mg), fraction of surfactant (0.5, 0.75 and 1 w/v %) and drug to lipid ratio (2, 4 and 6). Mean particle size and entrapment efficiency of the loaded Paromomycin were modeled statistically and the optimal condition was determined to approach to the maximum entrapment efficiency. The drug release profile of the optimal formulated material was examined in aqueous media and 64% of the Paromomycin loaded in SLNs was gradually released during 24 h, which reveals efficient prolonged release of the drug.

1. Introduction

Paromomycin, as a highly polar organic molecule, has a very low lipophilicity. It has a broad spectrum of activity against bacteria, cestodes, and protozoa, such as *Leishmania sp.* and has been prevalently used for the treatment of cutaneous leishmaniasis (CL). Leishmaniasis, which has diverse clinical manifestations, is caused by different species of Leishmania and is endemic in many countries (WHO, 2004). Although CL is a self-healing disease, but healing takes a long time, and healing times of even up to 2 years have been reported (Murray et al., 2005). The conventional topical dosage forms of Paromomycin have been tested in clinical trials for their activities against CL and showed promising results, but acceptable efficiency was not always seen (Asilian et al., 2003; Armijos et al., 2004). The formidable barrier nature of the Stratum Corneum (SC) of the skin does not allow the penetration of drugs with high hydrophilicities and molecular weights, like Paromomycin, which is observed in Fig. 1 (Ferreira et al., 2004). Furthermore, drugs topically applied for the treatment of CL must be able to target the Leishmania parasites within the phagolysosome of the infected macrophages in the deep dermal layer of the skin (Mauel, 1990; Asilian et al., 2003).

Solid lipid nanoparticles (SLNs) are colloidal carrier systems composed of a high melting point lipid/s as a solid core coated by surfactants. A clear advantage of SLNs is the fact that the lipid matrix is made from physiological lipids which decreases the danger of acute and chronic toxicity (Mandawgade and Patravale, 2008). SLNs have emerged as an alternative to other novel delivery approaches due to various advantages such as feasibility of incorporation of lipophilic and hydrophilic drugs, improved physical stability, low cost compared to liposomes and ease of scale-up and manufacturing (Mehnert and Mader, 2001). Moreover, the potential of SLNs in epidermal targeting, controlled release, negligible skin irritation, and protection of active compounds has been well established (Liu et al., 2007). In addition, the small particle sizes of SLNs ensure that the nanoparticles are in close contact with the SC, thus promoting the amount of the encapsulated agent which penetrates into the skin (Mei et al., 2003).

Loading of Paromomycin into SLNs can be problematic owing to its high hydrophilicity. Therefore, the objective of the present study is to evaluate the different variables affecting the entrapment efficiency of Paromomycin and particle size of SLN to achieve the maximum entrapment efficiency and the smallest particle size as possible.

Statistical design is the methodology of this research to project, select or establish the smaller number of experiments in such a

* Corresponding author. Tel.: +98 21 61112229; fax::+98 21 66957784.
** Co-corresponding author. Tel.: +98 21 66959057; fax: +98 21 66461178.
E-mail addresses: shfatemi@ut.ac.ir (S. Fatemi), vatanara@sina.tums.ac.ir (A. Vatanara).

0378-5173/$ – see front matter © 2011 Elsevier B.V. All rights reserved.
doi:10.1016/j.ijpharm.2011.12.037

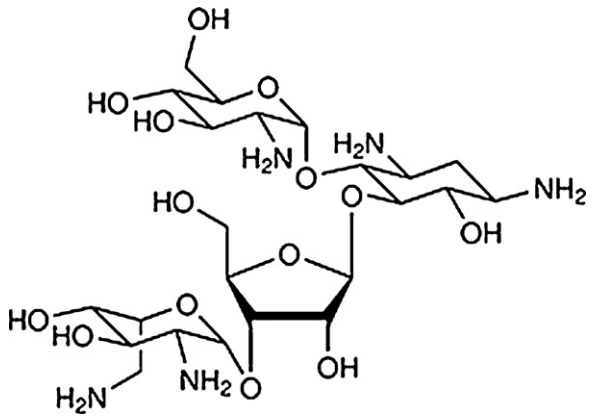

Fig. 1. Paromomycin chemical structure, molecular weight (base): 615.628 g/mole.

way that the required information is obtained from the most effective and precise way, carrying out the necessary experimentation (Lewis et al., 1999).

D-optimal design is one of the techniques in response surface method (RSM) which decreases the number of experiments when there are some categorical factors. D-optimal design has been adopted to optimize the liposomal formulation (Smistad et al., 2007) and self-emulsifying drug delivery systems (Basalious et al., 2010). Those studies demonstrated the advantage of D-optimal design in formulation and optimization of delivery systems.

In this study, two categorical factors such as SLNs preparation method and the type of lipid are studied for approaching to the best formulation; therefore D-optimal design is employed to have minimum number of experiments. D-optimal design of experiments allowed us to realize interactions among experimental variables within the studied range of variables, leading to better process conditions in addition to reducing the research time and cost (Box and Hunter, 1976).

2. Materials and methods

2.1. Materials

Paromomycin sulfate was purchased from Shenzhen Haorui, China. Tween 80, Span 85, stearic acid (SA), cetyl palmitate (CP), sodium sulfate, acetic acid, potassium hydroxide, boric acid, 2-mercaptoethanol, O-phthalaldehyde and sulfuric acid were purchased from Merck Co. Sodium 1-heptanesulfonate was purchased from Acros organic.

2.2. Preparation of Paromomycin loaded SLNs

2.2.1. Microemulsion technique

Lipid (stearic acid or cetyl palmitate) was heated to 85 °C. Surfactant was dispersed in the melted lipid until the dispersion appeared clear. The aqueous phase containing Paromomycin was heated to 85 °C and was added to the melted lipid under stirring. The resulted emulsion was subjected to high shear homogenizer (IKA Ultra-Turrax, T25, Germany) at 18,000 rpm for 20 min. The resulted nanoemulsion was immediately dispersed in cold double distilled water (2–5 °C) followed by stirring to solidify the nanoparticles (Mei et al., 2003).

2.2.2. Solvent diffusion technique

The desired amount of lipid was dissolved in 6 ml acetone in a water bath at 85 °C. An aqueous phase containing surfactant and Paromomycin was heated up to 85 °C and rapidly added into the stirred organic phase with agitation rate of 3000 rpm. The obtained emulsion was homogenized at 18,000 rpm for 20 min using high speed shear homogenizer. The resultant nanoemulsion was quickly added to stirring double distilled water at 2–5 °C and the nanoparticles were prepared (Hu et al., 2005).

Table 1
Levels of the factors in experimental design for preparation of Paromomycin loaded SLNs.

Parameters name	Levels		
	Numerical		
	−1	0	1
	Categorical		
	0		1
X_1 – lipid/drug ratio (L/D)	2	4	6
X_2 – surfactant percent (S) (w/v%)	0.5	0.75	1
X_3 – amount of drug (D), mg	60	90	120
X_4 – lipid type (LT)	Stearic acid	–	Cetyl palmitate
X_5 – method (M)	Microemulsion	–	Solvent diffusion

2.3. Statistical experimental design

A two-level fractional factorial design was performed and followed by D-optimal design to reduce the number of experiments and derive a proper quadratic model for the responses.

2.3.1. Fractional factorial design

Based on preliminary experiments the influential parameters such as; lipid/drug ratio (X_1), surfactant percent (X_2), amount of drug (X_3), type of lipid (X_4), stearic acid or cetyl palmitate, and method of SLNs preparation (X_5), microemulsion or solvent diffusion, were chosen as the variables to be studied (Table 1). Other parameters, i.e., homogenizing rate, homogenizing time and total volume of dispersion were set at fixed levels.

A two level half fractional factorial (2^{5-1}) design with two center points at each categorical factor was employed to identify the significant formulation and process variables affected on entrapment efficiency and mean particle size of SLNs. Detection of the curvature effect in the model was facilitated by adding center points and they were replicated to ensure the proper estimation of the pure experimental error.

This analysis is based on the assumption of a linear response of the standard factors, as given in following equation:

$$Y = B_0 + \sum_{i=1}^{5} B_i X_i + \sum_{i=1}^{5} \sum_{j=i+1}^{5} B_{ij} X_i X_j \quad (1)$$

Finally, an experimental plan with 24 experiments was made. Table 2 shows the standard order and the observed responses for five factors and 24 experiments. The experiments were performed in a random manner in order to avoid any systematic bias in the outcomes. The responses were obtained after each experimental run and they are observed in Table 2.

2.3.2. D-optimal design

The factorial design was augmented to D-optimal experimental design in the studied region of variables to derive the curvature effects of influential parameters. In this work, six experimental runs were generated and combined with fractional factorial design experiments (Table 2) to determine the quadratic relation of the effective parameters (Table 3).

The method of D-optimal design consisted of (i) defining levels, (ii) selection of the model that fits, and (iii) choosing design points, h, from the set of n candidate points generated according to the

Table 2
Half fractional factorial (2^{5-1}) design for preparation of Paromomycin loaded SLNs.

Run	Numeric factors			Categorical factors		Responses	
	X_1	X_2	X_3	X_4	X_5	Y_1 (%)	Y_2 (nm)
R_1	2	0.5	60	SA	SD	22.29	234.8
R_2	6	0.5	60	SA	ME	28.45	331.1
R_3	2	1	60	SA	ME	23.81	245.2
R_4	6	1	60	SA	SD	28.99	268.4
R_5	2	0.5	120	SA	ME	28.26	349.2
R_6	6	0.5	120	SA	SD	29.47	398.6
R_7	2	1	120	SA	SD	36.24	269.3
R_8	6	1	120	SA	ME	30.82	769.0
R_9	2	0.5	60	CP	ME	25.06	703.4
R_{10}	6	0.5	60	CP	SD	26.44	498.4
R_{11}	2	1	60	CP	SD	24.23	128.9
R_{12}	6	1	60	CP	ME	31.26	139.9
R_{13}	2	0.5	120	CP	SD	24.31	148.9
R_{14}	6	0.5	120	CP	ME	31.96	219.5
R_{15}	2	1	120	CP	ME	28.89	124.3
R_{16}	6	1	120	CP	SD	27.88	276.2
R_{17}	4	0.75	90	SA	ME	39.08	463.7
R_{18}	4	0.75	90	CP	ME	25.42	349.7
R_{19}	4	0.75	90	SA	SD	31.80	286.1
R_{20}	4	0.75	90	CP	SD	27.54	139.6
R_{21}	4	0.75	90	SA	ME	38.12	418.9
R_{22}	4	0.75	90	CP	ME	27.85	345.4
R_{23}	4	0.75	90	SA	SD	30.74	290.1
R_{24}	4	0.75	90	CP	SD	29.20	131.6

Lipid/drug ratio (X_1); surfactant percent (%w/v) (X_2); drug amount (mg) (X_3); lipid type (X_4); method (X_5); entrapment efficiency (%) (Y_1); particle size (nm) (Y_2); solvent diffusion (SD); microemulsion (ME); stearic acid (SA); cetyl palmitate (CP).

selected model. D-optimal design, as a technique, demands selection of the model at the beginning. In this particular case, there was some allusion about the model and a quadratic model was introduced as following:

$$Y_n = b_0 + b_1X_1 + b_2X_2 + b_3X_3 + \ldots + b_{12}X_1.X_2 + b_{13}X_1.X_3 + \ldots + b_{11}X_1^2 + b_{22}X_2^2 + b_{33}X_3^2 \quad (2)$$

where b_n is the coefficient associated with each nth factor, and the variables, X_1, X_2, X_3, X_4, and X_5 represent the factors of the model. Combination of factors (such as $X_1 \cdot X_2$) represents binary interactions between the individual factors.

The proposed model was evaluated for each response and the experimental data were analyzed statistically applying by the analysis of variance (ANOVA) using Design-Expert 6.0.6, a DOE software tool from Stat-Ease, Inc. The adequacy of the final model was verified by graphical and numerical analysis.

2.3.3. Optimization procedure

The simultaneous optimization technique popularized by Derringer and Suich was chosen for optimization of the responses (Derringer and Suich, 1980). This method is based on the utilization of desirability functions. Each response is converted into an individual desirability function d_i that can be varied over the range $0 < d_i < 1$. The design variables are then selected to maximize the overall desirability, Eq. (3):

$$D = (d_1 d_2 d_3 \ldots d_m)^{1/m} \quad (3)$$

where D is the overall desirability, d_i is the individual desirability and m is the number of responses(Montgomery, 2001). The target was improvement of formulation conditions to maximize the entrapment efficiency of hydrophilic drug, Paromomycin in SLNs and minimize the particle size. The lipid/drug ratio, surfactant percent, drug amount, lipid type and method were limited to the examined range of the experiments.

Table 3
Runs to augment the fractional factorial design to a D-optimal design.

Run	Numerical factors			Categorical factors		Responses	
	X_1	X_2	X_3	X_4	X_5	Y_1 (%)	Y_2 (nm)
R_{25}	4	0.5	60	CP	SD	31.26	446.1
R_{26}	4	1	120	CP	SD	36.34	298.7
R_{27}	6	0.75	60	CP	ME	31.01	398.7
R_{28}	6	1	90	SA	SD	34.10	433.6
R_{29}	2	0.5	90	SA	SD	32.03	320.8
R_{30}	2	0.75	120	CP	ME	31.23	314.6

Lipid/drug ratio (X_1); surfactant percent (%w/v) (X_2); drug amount (mg) (X_3); lipid type (X_4); method (X_5); entrapment efficiency (%) (Y_1); particle size (nm) (Y_2); solvent diffusion (SD); microemulsion (ME); stearic acid (SA); cetyl palmitate (CP).

2.4. Characterization of SLNs

2.4.1. Particles size measurement

The intensity weighted mean hydrodynamic size (called *z*-average) and the polydispersity index of the particles were measured by photon correlation spectroscopy (Zetasizer Nano Series, Malvern, UK) at 25 °C. Samples were diluted with double distilled water to a suitable concentration before the analysis of particle size.

2.4.2. Entrapment efficiency measurement

The supernatant was separated by centrifuging the SLNs dispersion at 26,000 rpm at −4 °C. The drug entrapment efficiency (EE) was calculated by Eq. (4):

$$\mathrm{EE} = \frac{W_1 - W_2}{W_1} \times 100 \quad (4)$$

where W_1 is amount of drug added in the formulation and W_2 is the amount of drug in supernatant.

2.4.3. HPLC analysis of Paromomycin

Paromomycin was analyzed using Waters series HPLC (Waters, USA). The column was Teknokroma, LICHROSPHER 100 RP8, C8 (150 mm × 46 mm) with 5 μm particles. The mobile phase consisted of aqueous 0.2 M Na_2SO_4, 1.2 mM sodium 1-heptanesulfonate and 0.1% acetic acid. The derivatization agent was prepared by O-phthalaldehyde and 2-mercaptoethanol in the methanol. The derivatization agent was introduced through a post-column tee at a flow rate of 1.0 ml min^{-1} with a Jusco PU-2086 plus pump. The combined derivatizing agent and column effluent proceeded into a stainless-steel reaction coil, wrapped in 3–5-cm coils. A fluorescence detector was connected to the effluent end of the coil: the xenon lamp pulsed at 20 Hz, and the excitation and emission monochromators, each with a 20-nm bandwidth, were set to wavelengths of 340 and 440 nm, respectively. Peak area data was collected with Chrom& Spec 1.5 software (Pick et al., 1997).

2.4.4. Drug release measurement

After prediction of the optimal conditions of Paromomycin loaded SLNs, drug release profile of the optimal formulation, with the highest entrapment efficiency, was studied by the dialysis bag method. Phosphate buffer (PBS, pH 7.4) was used as dissolution medium. The dialysis bag (molecular weight cutoff 12,000 Da) was soaked in DI water for 12 h before use. 5 ml of the prepared Paromomycin loaded SLNs dispersion was poured into the bag with the two ends fixed by clamps. The bags were placed in a conical flask and 50 ml dissolution media was added. The conical flasks were placed into a thermostatic shaker bath at 37 °C at a rate of 60 times per min. An aliquot of 0.5 ml dissolution medium was removed at a series of various points (0.5, 1, 2, 4, 8, 12 and 24 h) and the same volume of fresh dissolution medium was added accordingly. The drug content of the samples was analyzed by the HPLC method as described before.

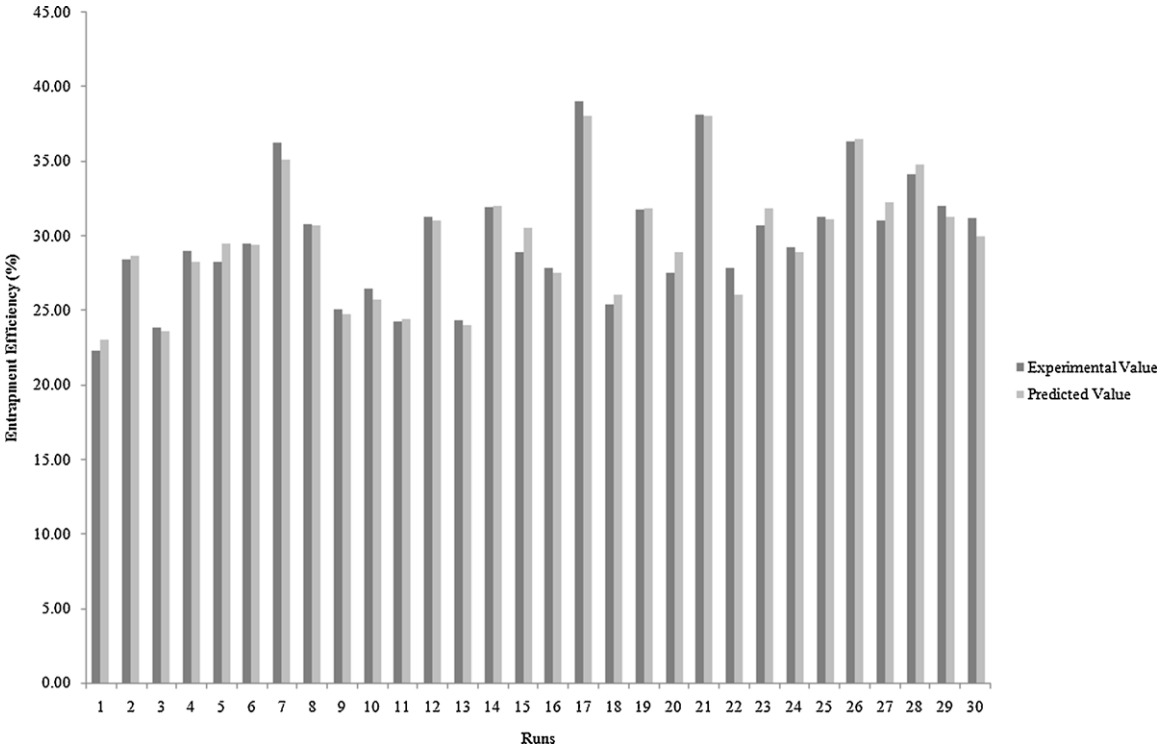

Fig. 2. The comparison between model and experimental value of entrapment efficiency.

Table 4
Analysis of variance: fractional factorial design.

Source	Responses	
	Y_1-entrapment efficiency	Y_2-particle size
p-value		
Model	<0.0001	<0.0001
Lack of fit	0.3561	0.171
Curvature	0.0049	0.5082
R^2 value	0.9968	0.9607

Table 5
ANOVA for the D-optimal design reduced quadratic model: entrapment efficiency.

Source	*p*-value	Source	*p*-value
Model	<0.0001	$X_1 \cdot X_5$	<0.0001
X_1	0.0002	$X_2 \cdot X_3$	0.052
X_2	<0.0001	$X_2 \cdot X_4$	0.0016
X_3	0.0068	$X_2 \cdot X_5$	<0.0001
X_4	<0.0001	$X_3 \cdot X_5$	<0.0001
X_5	<0.0001	$X_4 \cdot X_5$	<0.0001
$X_1 \cdot X_2$	0.0002	${X_1}^2$	0.0004
$X_1 \cdot X_4$	0.0008	R^2	0.9610

2.4.5. *Differential scanning calorimetry measurement*

Thermal behavior of raw materials and the optimum formulation of SLNs were studied quantitatively and qualitatively by differential scanning calorimetry (DSC 204 F1, Netzsch, Germany). The samples (7–12 mg) were accurately weighed into standard aluminum pans and sealed. Thermograms were recorded during heating and cooling runs at a scan rate of 10 °C min^{-1} between 25 and 400 °C.

3. Results and discussion

Thirty experimental runs were conducted using D-optimal design and two responses were determined as shown in Tables 2 and 3. The results of analysis of variance (ANOVA) are based on Fischer tests and calculated probability values (*p*-value) shown in Tables 4–7 for entrapment efficiency and particle size with 95% confident level. Since each of the independent variables exhibited

Table 6
Model equations in actual terms for each observed response.

Lipid type: stearic acid; method: microemulsion
$EE\% = 19.29 + 3.98 \times L/D + 53.29 \times S - 0.09 \times D - 3.33 \times L/D \times S - 0.09 \times S \times D - 0.57 \times (L/D)^2$
$PS = 1285.83 - 120.22 \times L/D - 1199.11 \times S - 8.76 \times D + 84.32 \times L/D \times S + 0.88 \times L/D \times D + 10.90 \times S \times D$
Lipid type: cetyl palmitate; method: microemulsion
$EE\% = 9.57 + 5.36 \times L/D + 43.36 \times S - 0.09 \times D - 3.33 \times L/D \times S - 0.09 \times S \times D - 0.57 \times (L/D)^2$
$PS = 2307.88 - 160.23 \times L/D - 1768.65 \times S - 14.62 \times D + 84.32 \times L/D \times S + 0.88 \times L/D \times D + 10.90 \times S \times D$
Lipid type: stearic acid; method: solvent diffusion
$EE\% = -3.93 + 6.65 \times L/D + 33.13 \times S + 0.14 \times D - 3.33 \times L/D \times S - 0.09 \times S \times D - 0.57 \times (L/D)^2$
$PS = 1014.55 - 81.33 \times L/D - 1199.11 \times S - 8.76 \times D + 84.32 \times L/D \times S + 0.88 \times L/D \times D + 10.90 \times S \times D$
Lipid type: cetyl palmitate; method: solvent diffusion
$EE\% = -5.12 + 8.03 \times L/D + 23.2 \times S + 0.14 \times D - 3.33 \times L/D \times S - 0.09 \times S \times D - 0.57 \times (L/D)^2$
$PS = 2036.60 - 121.33 \times L/D - 1768.65 \times S - 14.62 \times D + 84.32 \times L/D \times S + 0.88 \times L/D \times D + 10.90 \times S \times D$

EE%: entrapment efficiency; PS: particle size; *L*/*D*: lipid/drug ratio; *S*: surfactant percent; *D*: drug amount.

Table 7
ANOVA for the fractional factorial design: particle size.

Source	*p*-value	Source	*p*-value
Model	<0.0001	$X_1 \cdot X_3$	0.0027
X_1	0.0087	$X_1 \cdot X_4$	0.0137
X_2	0.0114	$X_1 \cdot X_5$	0.0158
X_3	0.9821	$X_2 \cdot X_3$	0.0001
X_4	0.0017	$X_2 \cdot X_4$	0.0003
X_5	0.0004	$X_3 \cdot X_4$	<0.0001
$X_1 \cdot X_2$	0.0104		

a significant effect on the responses, and entrapment efficiency revealed significant curvature effect, a higher order model was pursued. The following discussion centers on significant main factor effects and those of binary interactions on dependent variables as discovered by statistical analysis of the responses.

3.1. Entrapment efficiency

As described before, the entrapment efficiency of the hydrophilic drugs into SLNs is low; therefore one of the objectives was to evaluate the influenced parameters on entrapment efficiency. The statistical analysis of the data suggested that the fit of the model to the data was significant (p-value < 0.05) and resulted a good coefficient of determination (R^2 = 99.68%). Lack of fit was not significant (p-value > 0.05), indicating that the data can be described adequately by the introduced regression model (Table 4). Residuals were randomly distributed, ensuring absence of systematic error. As shown in Table 4, the curvature is significant in entrapment efficiency, which means there is at least one parameter with quadratic effect.

Firstly, a complete quadratic model containing the main variables, binary interactions and quadratic relations were proposed for entrapment efficiency, thereafter the nonsignificant terms were detected by ANOVA and ignored from the model, transforming the complete quadratic model to the reduced one. The resulted modified model of entrapment efficiency is described in Eq. (5):

$$Y_1 = b_0 + b_1X_1 + b_2X_2 + b_3X_3 + \beta_4X_4 + \beta_5X_5 + b_{12}X_1.X_2 + b_{23}X_2.X_3 + \beta_{14}X_1.X_4 + \beta_{15}X_1.X_5 + \beta_{24}X_2.X_4 + \beta_{25}X_2.X_5 + \beta_{35}X_3.X_5 + \beta_{45}X_4.X_5 + b_{11}X_1^2 \quad (5)$$

where β_{ij} represents coefficients of categorical factors or their interactions with numerical factors.

For the present model the p-values of the coefficients are determined by the Fischer test in ANOVA and the results are presented in Table 5. The p-values less than 0.05 imply that each term is significant. The reduced obtained model suggests the fit is well and about 96% of the experiments can be well fitted to the selected model (R^2 = 96%). A comparison between the model and experimental value of entrapment efficiency as a function of significant parameters for each thirty test runs can be observed in Fig. 2.

The residual analysis was employed to study the random behavior of the residuals, and normal probability plot was prepared for residual error of entrapment efficiency, as shown in Fig. 3. The plot of this figure is normally distributed and resembles a straight line. There is no severe indication of non-normality and neither any evidence pointing to possible outliers.

The second order polynomial regression equation of the entrapment efficiency in terms of coded factors is determined and presented in Eq. (6):

$$EE\% = 34.337 - 2.187X_1 + 4.166X_2 - 1.378X_3 - 3.693X_4 - 1.508X_5 - 1.663X_1.X_2 + 1.379X_1.X_4 + 2.664X_1.X_5 - 0.689X_2.X_3 - 1.241X_2.X_4 - 2.520X_2.X_5 + 3.400X_3.X_5 + 2.130X_4.X_5 + 2.302X_1^2 \quad (6)$$

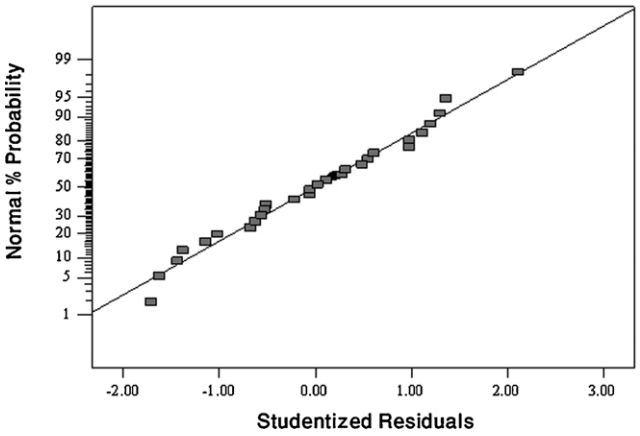

Fig. 3. Normal probability plot of residuals for Y_1, entrapment efficiency.

Coded equation is useful for identifying the relative significance of the factors by comparing the factor coefficients. Generally, in coded equation (Eq. (6)), positive coefficients indicate that a higher value is favorable for increasing the response, whereas the negative coefficients indicate that a lower level (lower amount) is desired. The magnitudes of the coefficients indicate the relative contributions of the factors into the response.

Because the effects from a number of two-factor interactions are statistically supported, the influence of the main effects on the entrapment efficiency cannot be considered, independently.

The effect of the formulation and process variables on a response can be evaluated by studying the response plots. From Fig. 4a–d, the response plots of entrapment efficiency as a function of drug amount and lipid/drug ratio, it can be seen that the effects of the parameters on the entrapment efficiency vary in different lipids and method types. As shown in Fig. 4a–d, lipid/drug ratio has quadratic effect and there is an optimum value with maximum entrapment efficiency. Increasing the lipid/drug ratio can afford more space to encapsulate drug under the condition of given surfactant concentration in the aqueous phase (Lv et al., 2009).

High concentration of Tween 80 results increasing the thickness of hydrophilic coating, and then more dispersion of drug in it (Lv et al., 2009). As shown in Eq. (6), lipid type and method have negative coefficients, indicating that the SLNs produced by microemulsion method have higher entrapment efficiency than the samples produced by solvent diffusion method and this result can be seen in Fig. 4a and b or Fig. 4c and d, comparatively. On the other hand, the entrapment efficiency of the cetyl palmitate SLNs is lower than stearic acid SLNs. Stearic acid is a self-emulsifying lipid and can entrap more hydrophilic drug in the particles. The lower entrapment efficiency of the cetyl palmitate may be due to its high crystalline structure (Lv et al., 2009) and the high crystalline order of nanoparticles could prevent incorporation of high amounts of drug molecules.

As shown in Eq. (6), the amount of drug coefficient is negative; it means that drug entrapment efficiency decreased with increasing the drug amount. But as described before, the amount of drug shows significant interactions with other factors, so it is concluded that the effect of drug amount is affected differently by the lipid type and the methods. As shown in Fig. 4a and b, increasing the drug amount causes decreasing the entrapment efficiency although in Fig. 4b and d the drug amount shows an inverse effect. You et al. (2007) have reported that the entrapment efficiency of vinorelbinebitartrate loaded SLNs was decreased by increasing the drug amount. Also, as shown in Fig. 4a and c, the trend of entrapment

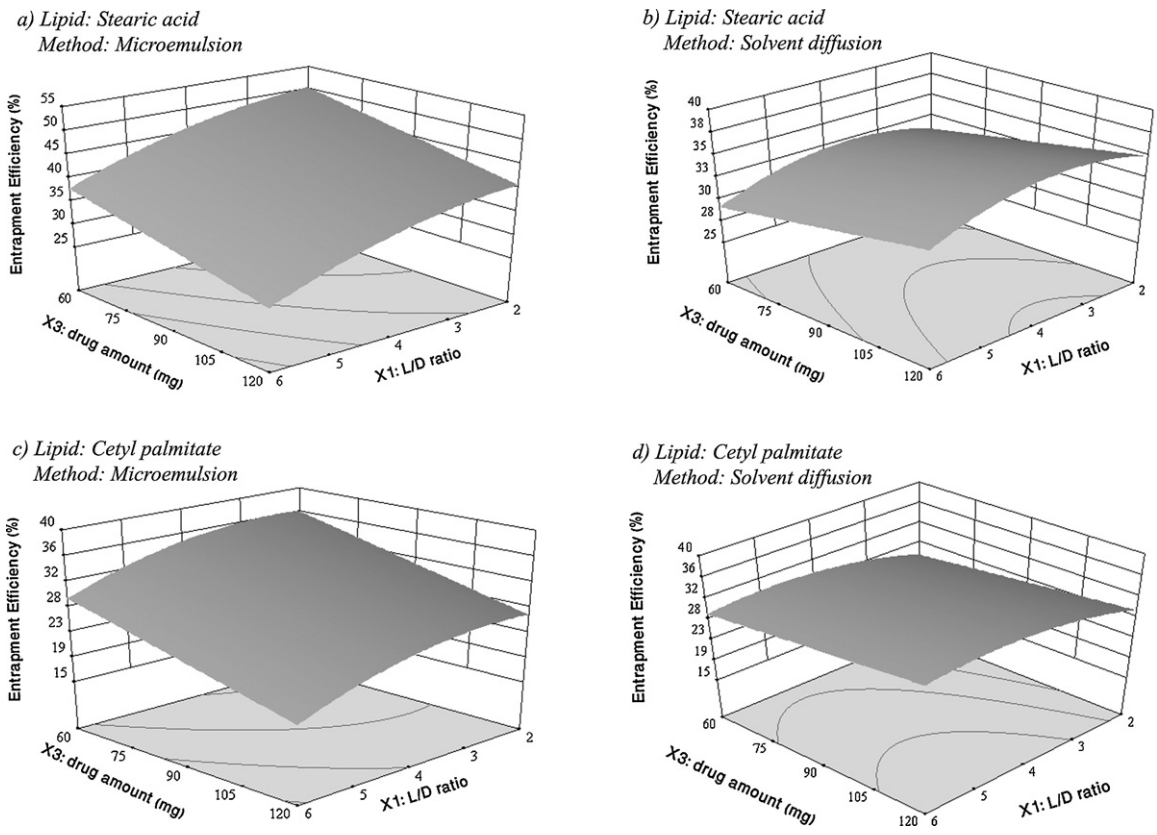

Fig. 4. Graphical interpretations of the entrapment efficiency models obtained for the (a) lipid: stearic acid, method: microemulsion; (b) lipid: stearic acid, method: solvent diffusion; (c) lipid: cetyl palmitate, method: microemulsion; (d) lipid: cetyl palmitate, method: solvent diffusion.

efficiency change for SLNs produced by microemulsion is identical in both lipid type, and also it is the same for SLNs produced by solvent diffusion (Fig. 4b and d). However the entrapment efficiency for SLNs produced by solvent diffusion method is less than microemulsion method.

Final response surface predictive models given in actual terms regarding response Y_1 (actual; entrapment efficiency – EE%) for different lipids types and different methods are stated in Table 6. Since each combination of categorical levels has an equation that predicts the response, four equations are presented for each response.

3.2. Particle size of SLNs

Small diameters of SLNs containing the Paromomycin could be a helpful factor in penetration of the Paromomycin into SC. The particle sizes obtained from the conducted experiments were determined in the range of 124–770 nm, indicating significant influence of formulation type and process variables on this response. The statistical analysis of the screened design data suggested that the proposed model was significant ($p < 0.05$) and resulted a pretty high coefficient of determination ($R^2 = 96.07\%$). Lack of fit was not significant ($p > 0.05$), indicating that the higher order interactions of the variables are not important (Table 4). Residuals were randomly distributed, ensuring the appropriateness of the mathematical model. As it has been shown in Table 4, the curvature was non-significant in the case of particle size. It means that none of quadratic effect of the variables is important in particle size of the SLNs. Comparison between the model and experimental particle size can be observed in Fig. 5, in which fairly agreement can be seen between model and experiments.

Fig. 6 presents a normal probability plot of residuals for the response, Y_2. There is no severe indication of non-normality and neither any evidence pointing to possible outliers. Normal probability plot presented in Fig. 6 resembles a straight line which shows normal distributed residuals.

As shown in Table 7, all of the variables except drug amount exhibit a statistically significant influence (p-value < 0.05) on the size of SLNs. Although the third factor, drug amount, was not statistically significant, it is retained in the model equation for hierarchical reasons. However, the amount of drug was involved in significant binary interactions with lipid/drug ratio, surfactant percent and lipid type. The effect of formulation type and process variables on particle size can be evaluated by observing Fig. 7a–d. The regression equation for the particle size in terms of coded factors is derived as Eq. (7):

$$PS = 319.070 + 43.570X_1 - 41.416X_2 + 0.308X_3 - 46.607X_4 - 57.848X_5 + 42.158X_1.X_2 + 52.883X_1.X_3 - 40.004X_1.X_4 + 38.895X_1.X_5 + 81.745X_2.X_3 - 71.191X_2.X_4 - X_2.X_5 - 88.016X_3.X_4 \quad (7)$$

As shown in Eq. (7), particle size has been increased by increasing the lipid/drug ratio and drug amount, but the effect of the drug amount is non-significant (p-value > 0.05). By increasing the lipid amount, the dispersion becomes more viscose and the exerted shear would not be enough for size reduction, therefore, the particles size tends to increase (Araujo et al., 2010). Increasing the particle size as a result of higher lipid amount may be occurred due to the lack of enough surfactant for covering the surface of the particles. This result confirms presence of interaction between lipid/drug ratio and surfactant concentration, in which the effect of the surfactant is dependent on the level of lipid/drug ratio.

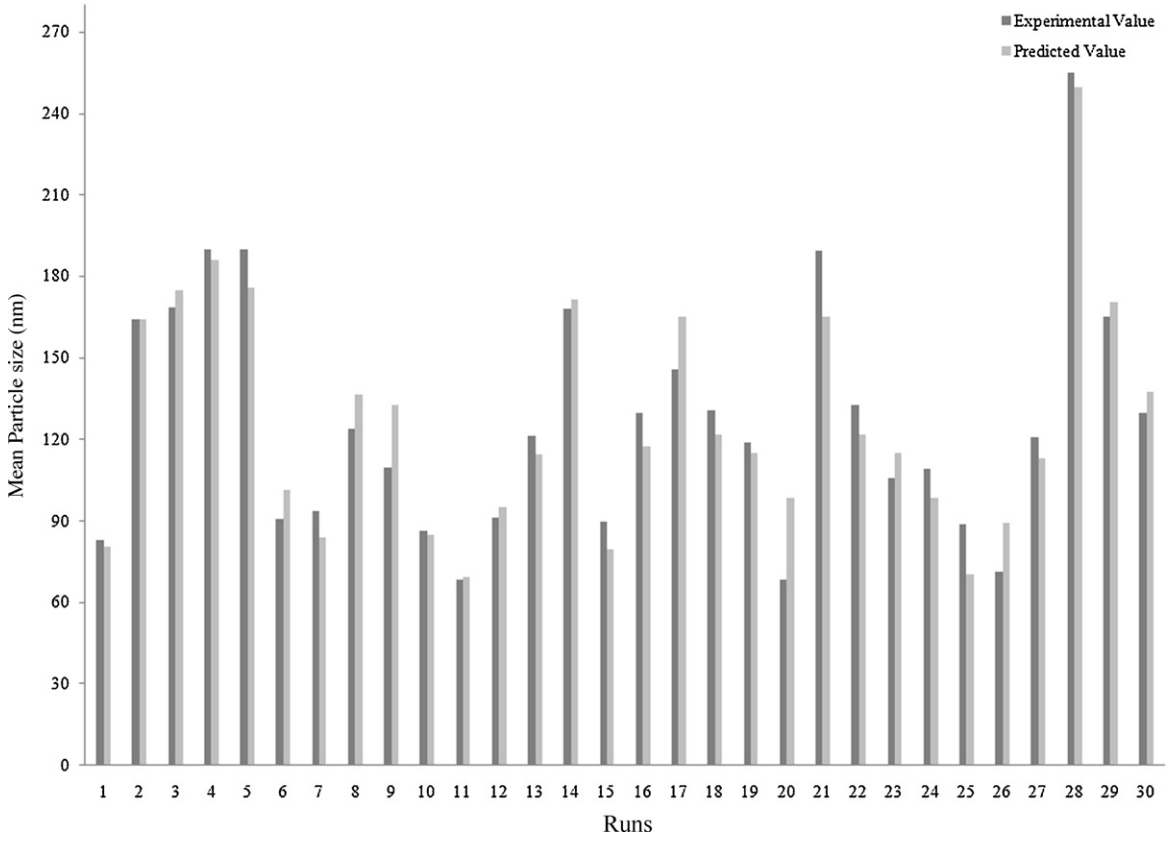

Fig. 5. The comparison between model and experimental value of mean particle size.

As can be seen in Eq. (7), surfactant has shown negative effect on particle size and by increasing the surfactant percent the particle size has been decreased (Fig. 7a–d). In fact, surfactant reduces interfacial tension and the lipid can become more homogenized in aqueous phase and causes reduction of particle size (Triplett and Rathman, 2009).

The results of statistical analysis revealed smaller particles produced by solvent diffusion compared to microemulsion method. In

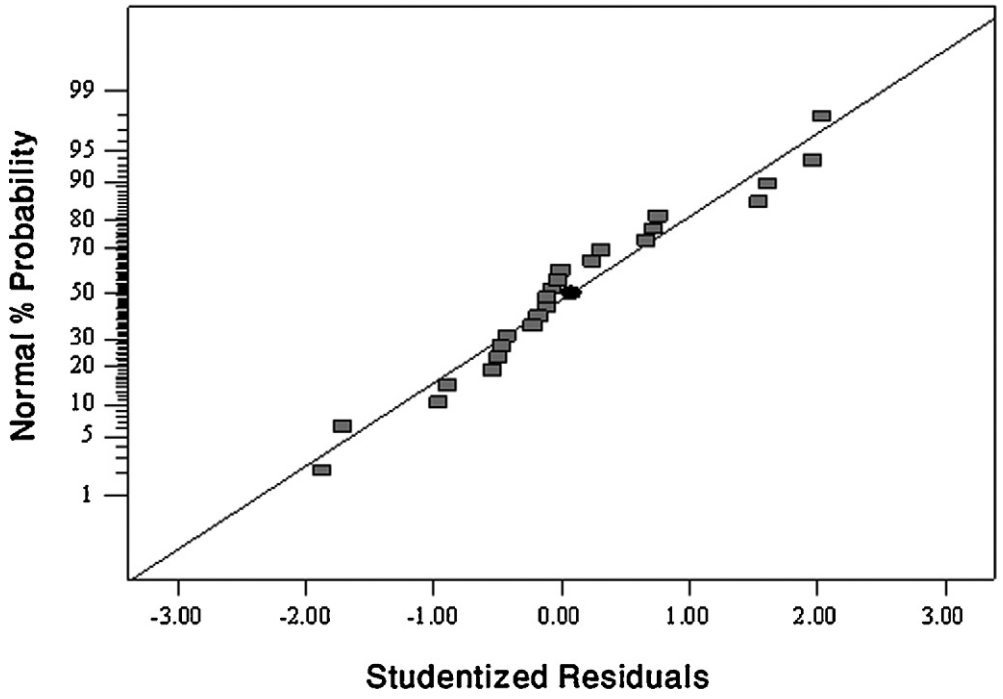

Fig. 6. Normal probability plot of residuals for Y_2, particle size.

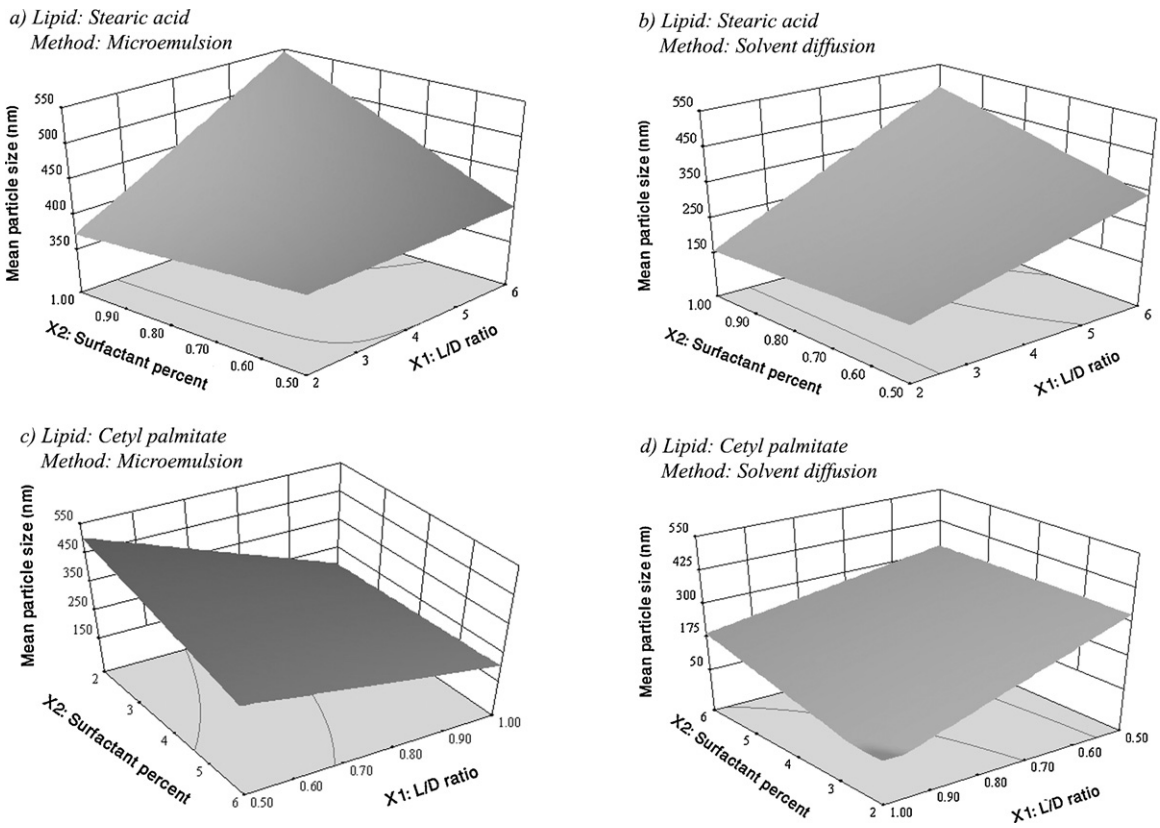

Fig. 7. Graphical interpretations of the particle size models obtained for the (a) lipid: stearic acid, method: microemulsion; (b) lipid: stearic acid, method: solvent diffusion; (c) lipid: cetyl palmitate, method: microemulsion; (d) lipid: cetyl palmitate, method: solvent diffusion.

solvent diffusion method, the lipid was dissolved in acetone and very small drops of the emulsion were formed after removing the acetone from dispersion phase. Therefore, the produced particles could have smaller diameters compared to the particles produced by microemulsion method (Yuan et al., 2007).

As can be seen in Eq. (7), the amount of drug has a positive coefficient which means raising the amount of drug enhances the particle size. It may be according to the incorporation of drug inside the particles and resulting incremental particle size (Liu and Wu, 2010), although this effect has not shown a significant effect in our analysis (p-value > 0.05).

As presented in Fig. 7a and b, by increasing the lipid amount and surfactant concentration in SLNs produced by stearic acid, particles size has been increased, that may be occurred due to hydrophobic attraction between particles whereas there is not enough surfactant in the dispersion to cover the surfaces of particles (Helgason et al., 2009).

On the contrary, in SLNs produced by cetyl palmitate, increasing surfactant concentration reduced particle size that it might occur due to the existence of mixed surfactants. In the SLNs produced by cetyl palmitate (HLB = 10), the mixture of Tween 80 (HLB = 15) and Span 85 (HLB = 1.8) was used in order to balance the HLB values of the aqueous and oily phases (Tween 80: Span 85, 7:3), on the other hand, Span 85 has smaller hydrophobic head compared to Tween 80, therefore the surface of the particles could be covered better by surfactants and aggregation of the particles might be prevented.

Mixed surfactant often can reduce interfacial tensions more than a single surfactant, particularly if the co-surfactant head group is significantly smaller than the surfactant head group. This phenomenon is largely due to an increased surfactant concentration at the interface, or surface excess which is made possible by minimization of repulsion forces by closely packed molecules, like surfactant (Fundarò et al., 2000).

A final response surface model given with actual units of the response Y_2 (actual particle size – PS) for different lipid types and different methods are stated in Table 6.

3.3. Optimal formulation

After generating the polynomial equations interpreting the dependent and independent variables, the formulation was optimized for the two responses: entrapment efficiency and particle size. The optimal values of the variables were obtained by the direct search method and numerical analyses based on the criterion of desirability functions. The optimized factor values were derived by minimizing particle size and maximizing entrapment efficiency. The optimal formulation was predicted in the level of lipid/drug ratio: 4, surfactant percent: 0.75%, amount of drug: 90 mg, using stearic acid and microemulsion method. To confirm the reliability of the response surface model, the SLNs with the optimized factor levels were prepared and evaluated. The experimental results were in a good agreement with the predicted values, as shown in Fig. 8, which confirmed the predictability and validity of the model. Finally, the drug release and thermal behavior of the optimum formulation was investigated for drug delivery, in a buffer solution.

3.4. In vitro drug release

A key issue investigated in this study was the feasibility of using lipid nanoparticles to deliver Paromomycin. The ability of nanoparticles to deliver Paromomycin was examined by determining the drug release, as shown in Fig. 9. The amount of Paromomycin released from the SLNs was plotted as a function of time. The release

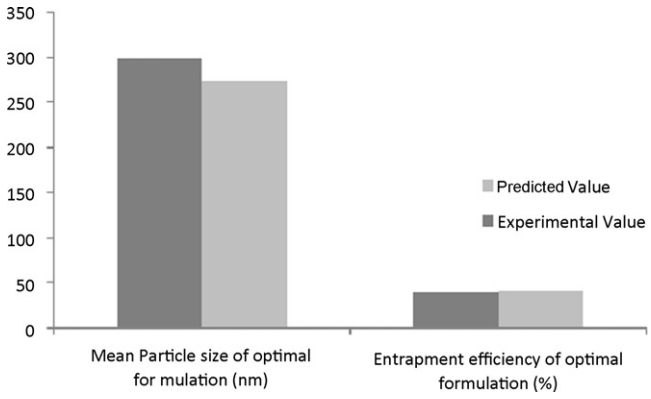

Fig. 8. Validation of the predicted optimal results, with experimental value.

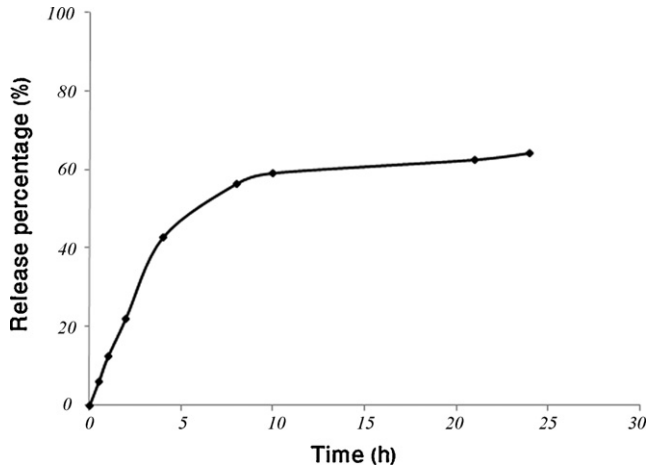

Fig. 9. In vitro release kinetics of Paromomycin loaded SLNs, as determined by dialysis method.

profile indicated that SLNs dispersion showed a retarded release of the hydrophilic drug in which 64% of Paromomycin was released after 24 h.

Release kinetic from the optimum formulation of SLNs was modeled using the Korsmeyer–Peppas law (Eq. (8)) (Peppas, 1985):

$$\frac{M_t}{M_\infty} = kt^n \quad (8)$$

where M_t/M_∞ is the fractional release of drug after time t, k is a constant that incorporates the geometric characteristics of the release device and n is the release exponent. The value of n is a parameter that is descriptive for the shape of the curve. It has been interpreted as drug release by Fickian diffusion ($n = 0.5$), Case II ($n = 1$) or a mechanism in which both diffusion and erosion play significant roles ($n = 0.5 < n < 1.0$) (Peppas, 1985). In fact, drug release is more complex than this simple model although significant changes of this parameter can change the curve shape which would indicate a significant shift in the drug release mechanism.

The value of n was obtained 0.59 and the profile of the drug release from SLNs would be the mixture of diffusion and erosion. The other information of the model is presented in Table 8. You

Table 8
Kinetic parameters of Korsmeyer–Peppas law for in vitro drug release of optimal formulation of SLNs.

$\frac{M_t}{M_\infty} = kt^n$	R^2 [a]	0.913
	k	0.184
	n	0.59

[a] Coefficient of determination.

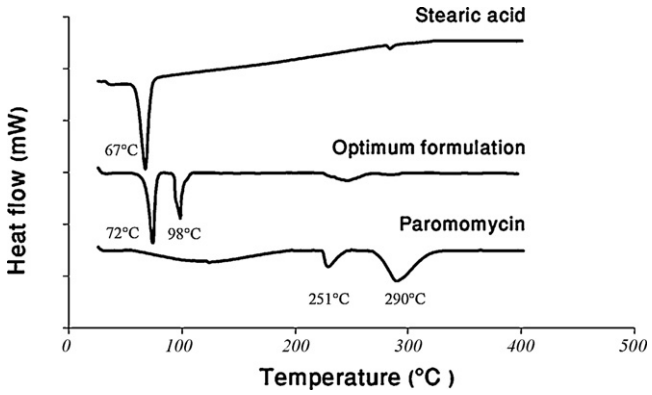

Fig. 10. DSC thermograms of pure Paromomycin sulfate, stearic acid and Paromomycin loaded SLNs.

et al. (2007) reported that the corrosion of lipid materials could be one of the mechanisms of drug release.

3.5. Results of DSC

DSC analysis of stearic acid, Paromomycin sulfate and optimum formulation of Paromomycin loaded SLNs are presented in Fig. 10. Endothermic peak of melting point of pure stearic acid was detected at 67 °C. By entrapping the Paromomycin into stearic acid SLNs, the melting point of the mixture was shifted to 72 °C; it is due to stearic acid alteration to β crystal state with the lowest energy configuration. At 251 °C and 290 °C, two endotherms indicate the Paromomycin sulfate decomposition in optimum formulation and pure Paromomycin (Arcamone et al., 1977; Wahlig et al., 1986) which are related to the existence of two types of Paromomycin (type I and type II). A peak was detected at 98 °C that could be related to evaporation of water entrapped in the formulation.

4. Conclusions

Formulation and preparation of Paromomycin loaded SLNs have been done and statistical design, analysis and modeling have been applied to predict the entrapment efficiency and particle size for two types of lipids, stearic acid and cetyl palmitate, two kinds of methods, microemulsion and solvent diffusion. The effect of three numerical variables, lipid/drug ratio, surfactant fraction and drug amount with their interactions have been evaluated and modeled.

The best local maximum of entrapment efficiency (41.65%) was found at lipid/drug ratio: 4, surfactant percent: 0.75%, drug amount: 90 mg, lipid type: stearic acid and microemulsion method. The release profile of the produced SLN was investigated in aqueous media and it showed prolonged release during 24 h, up to 64% release.

Acknowledgements

This work was partially supported by Tehran University of Medical Sciences. The authors would like to thank Dr. Mohsen Amini for his assistant.

References

Araujo, J., Gonzalez-Mira, E., Egea, M.A., Garcia, M.L., Souto, E.B., 2010. Optimization and physicochemical characterization of a triamcinolone acetonide-loaded NLC for ocular antiangiogenic applications. Int. J. Pharm., doi:10.1016/j.ijpharm.2010.03.034.

Arcamone, M., Guiseppe, Cassinelli, V., 1977. Paromomycin derivatives and process for the preparation thereof. US patent 4,021,601.

Armijos, R.X., Weigel, M.M., Calvopina, M., Mancheno, M., Rodriguez, R., 2004. Comparison of the effectiveness of two topical Paromomycin treatments versus

meglumineantimoniate for New World cutaneous leishmaniasis. Acta Trop. 91, 153–160.
Asilian, A., Jalayer, T., Nilforooshzadeh, M., Ghassemi, R.L., Peto, R., Wayling, S., 2003. Treatment of cutaneous leishmaniasis with aminosidine (Paromomycin) ointment: double-blind, randomized trial in the Islamic Republic of Iran. Bull. WHO 81, 353–359.
Basalious, E.B., Shawky, N., Badr-Eldin, S.M., 2010. SNEDDS containing bioenhancers for improvement of dissolution and oral absorption of lacidipine. I. Development and optimization. Int. J. Pharm., doi:10.1016/j.ijpharm.2010.03.008.
Box, G., Hunter, J., 1976. Statistics for Experiments. John Wiley & Sons, New York.
Derringer, G.C., Suich, R., 1980. Simultaneous optimization of several response variables. J. Qual. Technol. 12, 214–219.
Ferreira, L.S., Ramaldes, G.A., Nunan, E.A., Ferreira, L.A.M., 2004. In vitro skin permeation and retention of Paromomycin from liposomes for topical treatment of the cutaneous leishmaniasis. Drug Dev. Ind. Pharm. 30, 289–296.
Fundarò, A., Cavalli, R., Bargoni, A., Vighetto, D., Zara, G.P., Paolo, G., Gasco, M.R., 2000. Non-stealth and stealth solid lipid nanoparticles carrying doxorubicin: pharmacokinetics and tissue distribution after i.v. administration to rats. Pharmacol. Res. 42, 337–343.
Helgason, T., Awad, T.S., Kristbergsson, K., McClements, D.J., Weiss, J., 2009. Effect of surfactant surface coverage on formation of solid lipid nanoparticles (SLN). J. Colloid Interface Sci. 334, 75–81.
Hu, F.Q., Jiang, S.P., Du, Y.Z., Yuan, H., Ye, Y.Q., Zeng, S., 2005. Preparation and characterization of stearic acid nanostructured lipid carriers by solvent diffusion method in an aqueous system. Colloids Surf. B: Biointerfaces 45, 167–173.
Lewis, G.A., Mathieu, D., Phan-Tan-Luu, R., 1999. Pharmaceutical Experimental Design. Marcel Dekker, New York.
Liu, C.H., Wu, C.T., 2010. Optimization of nanostructured lipid carriers for lutein delivery. Colloids Surf. A: Physicochem. Eng. Asp. 353, 149–156.
Liu, J., Hu, W., Chen, H., Ni, Q., Xu, H., Yang, X., 2007. Isotretinoin-loaded solid lipid nanoparticles with skin targeting for topical delivery. Int. J. Pharm. 328, 191–195.
Lv, Q., Yu, A., Xi, Y., Li, H., Song, Z., Cui, J., Cao, F., Zhai, G., 2009. Development and evaluation of penciclovir-loaded solid lipid nanoparticles for topical delivery. Int. J. Pharm. 372, 191–198.
Mandawgade, D.S., Patravale, V.B., 2008. Development of SLNs from natural lipids: application to topical delivery of tretinoin. Int. J. Pharm. 363, 132–138.
Mauel, J., 1990. Macrophage parasite interactions in Leishmania infections. J. Leukoc. Biol. 47, 187–193.
Mehnert, W., Mader, K., 2001. Solid lipid nanoparticles production, characterization and applications. Adv. Drug Deliv. Rev. 47, 165–196.
Mei, Z., Chen, H., Wang, T., Yang, Y., Yang, X., 2003. Solid lipid nanoparticle and microemulsion for topical delivery of triptolide. Eur. J. Pharm. Biopharm. 56, 189–196.
Montgomery, D.C., 2001. Design and Analysis of Experiments. Wiley & Sons, New York.
Murray, H.W., Berman, J.D., Davies, C.R., Saravia, N.G., 2005. Advances in leishmaniasis. Lancet 366, 1561–1577.
Peppas, N.A., 1985. Analysis of Fickian and non-Fickian drug release from polymers. Pharm. Acta Helv. 60, 110–111.
Pick, J., Olson, L., Ellis, W., Lim, P., 1997. Development and validation of a method to extract and quantitate Paromomycin and gentamicin from an aquaphilic cream formulation. J. Pharm. Biomed. Anal. 16, 131–137.
Smistad, G., Jacobsen, J., Sande, S.A., 2007. Multivariate toxicity screening of liposomal formulations on a human buccal cell line. Int. J. Pharm. 330, 14–22.
Triplett, M.D., Rathman, J.F., 2009. Optimization of b-carotene loaded solid lipid nanoparticles preparation using a high shear homogenization technique. J. Nanopart. Res. 11, 601–614.
Wahlig, H., Dingeldein, E., Kirchlechner, R., 1986. Flavonoid phosphate salts of aminoglycoside antibiotics. US patent 4,617,293.
World Health Organization, 2004. Scientific Working Group on Leishmaniasis. Meeting Report. World Health Organization, Geneva, Switzerland.
You, J., Wan, F., Cui, F., Sun, Y., Du, Y., Hu, F., 2007. Preparation and characteristic of vinorelbinebitartrate-loaded solid lipid nanoparticles. Int. J. Pharm. 343, 270–276.
Yuan, H., Huang, L.F., Du, Y.Z., Ying, X.Y., You, J., Hu, F.Q., Zeng, S., 2007. Solid lipid nanoparticles prepared by solvent diffusion method in a nanoreactor system. Colloids Surf. B: Biointerfaces 61, 132–137.